

Weak Lensing Observations of High-Redshift Clusters of Galaxies

D. Clowe

*Max-Planck-Institut für Astrophysik, Karl-Schwarzschild-Str. 1,
D-85748 Garching, Germany*

G. Luppino, N. Kaiser, and I. Gioia

*Institute for Astronomy, University of Hawaii, 2680 Woodlawn Drive,
Honolulu, HI 96822*

Abstract. We present results of a weak gravitational lensing survey of six X-ray selected high-redshift clusters of galaxies. We find that the masses of the clusters derived from weak lensing are comparable to those derived from the X-ray observations. We show that many of the clusters have significant substructure not observed in the X-ray observations and that for the more massive clusters a singular isothermal sphere does not provide a good fit to the radial mass profile.

1. Introduction

High-redshift clusters of galaxies are very powerful tools for testing cosmological and structure formation models. Both the expected number density of massive clusters at $z > 0.5$ and the amount of substructure contained within the clusters depend very strongly on the mass density of the universe (Bahcall, Fan, & Cen 1997). X-ray observations have proven to be a very efficient means to detect these clusters. Unlike optical surveys, in which one can find an overdensity which is a superposition of unrelated galaxies, clusters are detected in X-rays emitted from gas heated during infall into a large potential well. While masses derived from the X-ray observations have been used to apply constraints to cosmological models (Henry 1997), they are subject to an uncertainty in that they, like dynamical mass estimates from cluster galaxy redshifts, depend on an assumed dynamical state of the cluster (Evrard, Metzler, & Navarro 1996). Weak gravitational lensing, however, has no such dependence, and thus can, in theory, provide mass estimates independent of any assumptions regarding the cluster lens.

We, therefore, have undertaken an optical survey of high-redshift, X-ray selected clusters of galaxies to perform a weak lensing analysis on the clusters. Our primary goals are to measure the masses of the clusters without assumptions regarding the degree of virialization of the clusters and to detect any substructure in the clusters which would be indicative of the clusters still undergoing initial formation. We have, to date, observed six $z > 0.5$ clusters, five from the Einstein Medium Sensitivity Survey (Gioia & Luppino 1994) and one from the ROSAT

North Ecliptic Pole survey (Henry *et al.* 1998). All six clusters have deep (> 1.5 hours) exposures in R -band from the Keck Observatory as well as shallower I - and B -band images from the UH88" telescope.

2. Weak Lensing Analysis

A weak lensing signal is detected in a field by measuring the ellipticities of background galaxies and looking for a statistical deviation from an isotropic ellipticity distribution. We used a hierarchical peak finding algorithm on the R -band images to detect faint galaxies and measure their magnitudes and second moments of the flux distribution. The second moments were used to calculate ellipticities for each object, which were then corrected for psf anisotropies and reduction of the ellipticity due to psf smearing using techniques originally developed in Kaiser, Squires, & Broadhurst (1993). Details of the data reduction process can be found in Clowe *et al.* (1999) and a review of these and other techniques can be found in Mellier (1999).

Once the ellipticities are corrected for psf smearing they can be used to measure the shear caused by the gravitational lensing exerted by the cluster. The shear field is quite noisy because of the intrinsic ellipticity distribution of the background galaxies, which is the dominant source of random error in weak lensing analysis. The shear can then be converted to the convergence, κ , which is the surface mass density of the lens divided by Σ_{crit} , where

$$\Sigma_{crit} = \frac{c^2}{4\pi G} \frac{D_{os}}{D_{ol}D_{ls}}. \quad (1)$$

The D 's are angular distances between the observer, the lens (cluster), and the source (background galaxy). For low redshift clusters ($z < 0.3$), Σ_{crit} is effectively constant for $z_{bg} > .8$, where most background galaxies are located. For high redshift clusters, however, one must know the redshift distribution of the background galaxies to convert the convergence to a surface density. As the redshift distribution of the galaxies used in our sample ($23 < R < 26.5$ and $R - I < 0.9$) is currently poorly known, we cannot give a definite measure of the mass for these clusters. If the mass of the clusters can be measured by some other means, however, then one can measure the mean redshift, and possibly the redshift distribution, of the background galaxies. We have done this (Clowe *et al.* 2000) and find good agreement between the mean redshift we measure and the mean redshift calculated from the Fontana *et al.* (1999) HDF-S photometric redshift estimates, using the same magnitude and color selection criteria.

We have used two different methods to convert shears to convergences. The first method is the KS93 inversion algorithm (Kaiser & Squires 1993) which uses the fact that both the shear and the convergence are combinations of second moments of the surface potential to transform, in Fourier space, between the two. This results in a two-dimensional image of the convergence, and thus the surface density, of the clusters but is limited in that it can only determine the convergence to an unknown additive constant. The second method, aperture densitometry, measures the circularly-averaged radial profile of the convergence around an arbitrarily chosen center minus the average convergence of a chosen annular region, usually set at the edges of the image. One can then either assume

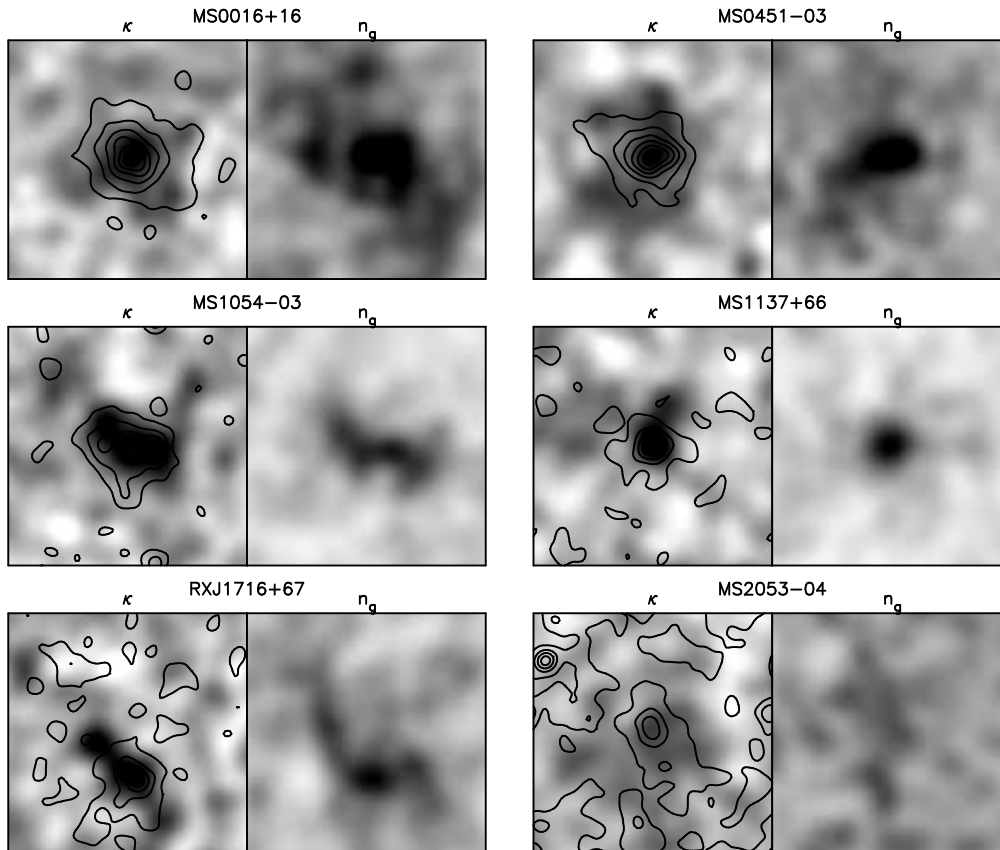


Figure 1. Above are maps of the mass reconstruction (left), using the KS93 algorithm, and number density of cluster galaxies as selected by $R - I$ color (right) for all of the clusters in the survey. Plotted in contours overlayed on the mass reconstructions are X-ray images of the field from the ROSAT PSPC. All the images have been smoothed by the same scale, and the greyscale is the same for every cluster.

the convergence in this outer region is zero and measure a minimum mass at a given radius or fit the profile with an assumed mass model and determine the average convergence in the annular region for the model.

3. Discussion

The maps of the convergence are given in Figure 1, along with contour overlays of the ROSAT X-ray emission and maps of the number density of galaxies with colors similar to the brightest cluster galaxy. As can be seen, there is in general a very good agreement between the features present in the galaxy number density distribution and the mass reconstructions. Most of these features are, however, at moderate statistical significance in the mass reconstructions, and their shapes have probably been altered to a large degree by the noise in the re-

Table 1. Cluster Sample

Cluster	z	T_X keV	M (500 kpc) $h^{-1}10^{14}M_\odot$	M/L (500 kpc) hM_\odot/L_\odot	SIS $\chi^2/(n-1)$	NFW $\chi^2/(n-2)$	F-test %
MS0016+16	0.547	8.4	4.1	260	1.08	0.93	85
MS0451-03	0.550	10.4	7.9	480	1.61	1.32	97
MS1054-03	0.826	12.3	12.7	590	1.33	0.94	99.5
MS1137+67	0.783	5.7	6.1	670	1.13	1.16	-
MS2053-04	0.586	8.1	3.0	360	0.99	1.00	-
RX1716+67	0.809	6.7	3.8	350	1.00	1.03	-

constructions. In particular, three of the clusters have a secondary peak in both the mass and galaxy surface densities. For two of these clusters, MS1054–03 and RXJ1716+67, spectra of the galaxies in the peaks have shown that they are at the same redshift as the main cluster peak (Tran *et al.* 1999; Gioia *et al.* 1999), while insufficient numbers of spectra exist for MS2053–04 to determine if the second peak is physically associated with the cluster.

Using the aperture densitometry profiles, assuming the center of each cluster is the position of the brightest cluster galaxy, we have calculated the best fit singular isothermal sphere and NFW profiles (Navarro, Frenck, & White 1996). This was done using a χ^2 fitting algorithm and using the mean redshift of the HDF-S photometric redshift catalog for galaxies with the same magnitude and color range as the selected background galaxies. We find that the isothermal sphere model is a good fit to the lower mass clusters, but a poor fit to the higher mass clusters. The NFW profiles, however, provide a good fit to all the clusters, although the best fit profiles do not follow the relationship between total mass and concentration as given by the zero redshift relaxed N-body clusters in Navarro, Frenck, & White (1996). Using an F-test, we have determined that the difference in the reduced χ^2 for the two fits in the most massive clusters is significant in the 2-3 σ range. Masses for the clusters measured at a 500 h^{-1} kpc radius from the BCG are given in table 1, along with the mass-to-light ratio at the same radius using the luminosity of galaxies with colors similar to the BCG to calculate the cluster luminosity.

We are currently investigating statistics which can be used to quantify the amount of substructure present in the mass reconstructions. One statistic which we have tried is measuring the ellipticity of the mass peaks from their second moments of the surface density. To do this, however, we first must assume a value for the additive constant for each reconstruction. We have chosen this value so that the mean convergence in an annular region located 2/3rds of the distance from the center to the nearest edge in the image is the same as the mean convergence in the best fit NFW profile to each cluster. We then measure the second moments using a Gaussian weighting function with a FWHM of 100 h^{-1} kpc. Ellipticities measured in this manner are extremely sensitive to the value of the added constant, and changing the constant from the maximum to minimum value allowed within the 1σ NFW profiles from the aperture densitometry fits would often change the measured ellipticity by a factor of two.

To determine the significance of these ellipticities we performed Monte-Carlo simulations in which background galaxies were randomly positioned in a field with the same number density as seen in the images. These galaxies were then sheared and displaced appropriately for an isothermal sphere of mass similar

to that measured in the clusters. A mass reconstruction was then performed on the galaxy distribution and the ellipticity of the central peak was measured. As the isothermal spheres have a zero ellipticity, any ellipticity measured is induced by the noise in the reconstruction from the intrinsic ellipticity distribution of the galaxies. From this distribution, we determined that the minimum ellipticities measured above for MS1054, RXJ1716, and MS0451 are greater than 72%, 88%, and 92% of the simulations. The other clusters have ellipticities consistent with those induced by noise.

A second statistic we have investigated is that of the separation between the centroid of the mass distribution in the reconstruction, measured from minimizing the first moment of the mass distribution, and the position of the brightest cluster galaxy. To determine the significance of the separations we used the same Monte-Carlo simulations as above and measured the separation in centroid of the reconstructed mass distribution and that used when shearing the galaxies. From this we find that separation seen in RXJ1716 is larger than 98% of the simulations, but that none of the other clusters has a significant separation.

Acknowledgments. We wish to thank Pat Henry, Harald Ebeling, Chris Mullis, and Megan Donahue for sharing their X-ray data prior to publication. This work was supported by NSF Grant AST-9500515 and the “Sonderforschungsbereich 375-95 für Astro-Teilchenphysik” der Deutschen Forschungsgemeinschaft.

References

- Bahcall, N. A., Fan, X., & Cen, R. 1997, *ApJ*, 485, L53
 Clowe, D., Luppino, G., Kaiser, N., & Gioia, I. 1999, *ApJ*, in press
 Clowe, D., Luppino, G., & Kaiser, N. 2000, in prep
 Evrard, A. E., Metzler, C. A., & Navarro, J. F. 1996, *ApJ*, 437, 56
 Fontana, A., D’Odorico, S., Fosbury, R., Giallongo, E., Hook, R., Polli, F., Renzini, A., Rosati, P., Viezzer, R. 1999, *A&A*, 343, L19
 Gioia, I. M. & Luppino, G. A. 1994, *ApJS*, 94, 583
 Gioia, I.M., Henry, I.M., Mullis, C.R., Ebeling, H. and Wolter, A. 1999, *AJ*, 117, 2608
 Henry, J. P. 1997, *ApJ*, 489, L1
 Henry, J. P., Gioia, I. M., Mullis, C. R., Clowe, D. I., Luppino, G. A., Boehringer, H., Briel, U. G., Voges, W., & Huchra, J. P. 1997, *AJ*, 114, 1293
 Kaiser, N., Squires, G., & Broadhurst, T. 1995, *ApJ*, 449, 460
 Kaiser, N. & Squires, G. 1993, *ApJ*, 404, 441
 Mellier, Y. 1999, *ARA&A*, in press
 Navarro, J. F., Frenk, C. S., & White, S. D. M. 1996, *ApJ*, 462, 563
 Tran, K., Kelson, D., Van Dokkum, P., Franx, M., Illingworth, G., Magee, D. 1999, *ApJ*, 522, 39